https://doi.org/10.17221/46/2025-RAE

Detection of heat-stressed chickens in poultry house based on deep network and optical flow vectors in the Fourier domain

*Ngo Quoc Viet, Thai Yen**

Faculty of Information Technology, Ho Chi Minh City University of Education, Ho Chi Minh City, Vietnam

**Corresponding author: ttkyen2003@gmail.com*

Citation: Viet N.Q., Yen T. (2025): Detection of heat-stressed chickens in poultry house based on deep network and optical flow vectors in the Fourier domain. Res. Agr. Eng., 71: 189–199.

Abstract: The productivity and quality of the entire flock are negatively impacted by heat stress in chickens, which can have major repercussions, particularly in crowded farming settings where diseases are easy to spread and hard to control. This study uses deep networks and optical flow to identify heat stress in chickens. The technique focuses on identifying obvious signs of heat stress, such as panting and open-mouth breathing in chickens. There are two phases to the suggested approach: (1) using a deep network to detect open-mouth breathing in chickens; (2) using the Gunnar Farnebäck algorithm to compute the optical flow vectors of the wattle, the breathing frequency is estimated in the Fourier domain for the detection of panting chickens. The proposed method was tested on the obtained dataset and demonstrated its ability to recognise heat-stressed chickens in crowded conditions, achieving an overall performance metric of 0.90 by integrating the results of both phases. The two-phase approach, which incorporates the open-mouth breathing behaviour and panting frequency, improves the efficiency and assures robust, reliable heat stress detection.

Keywords: animal welfare; Fourier transform; motion estimation; panting detection; thermal stress

Poultry farming is essential to the world's food supply chain and makes a substantial contribution to global economic growth. The demand for eggs is predicted to rise by 40% and the demand for chicken meat is predicted to double by 2050 (Franzo et al. 2023). In the poultry business, product quality plays a role in both satisfying consumer demand and generating revenue for farmers. Other chickens in the flock may be impacted when a small number of them exhibit strange behaviour. In intensive farming settings, like chicken farms, where sizable flocks are usually raised in cramped quarters, this is particularly crucial. As a result, careful observation and management of the flock's health has become crucial to guaranteeing the effectiveness and quality of the egg production.

In chickens, heat stress is a worryingly aberrant health condition (Figure 1). Heat stress negatively affects the health of hens and the quality of their eggs, according to numerous research studies. Chickens under heat stress have slower growth, poorer immune systems, greater mortality rates, and faster breathing rates. According to Abbas et al. (2022), heat stress causes chickens to become less active, which, in turn, causes them to eat less, which leads to nutrient shortages, acid-base imbalances, and altered gene functioning. According to the study by Kim et al. (2024), hens under persistent heat stress showed decreased egg production and quality over a four-week period. The majority of the chickens in poultry houses are usually impacted by ambient variables that cause heat stress, and very seldom are a small number of individual chickens affected. For farmers to effectively intervene, manage, and regulate livestock quality while averting

https://doi.org/10.17221/46/2025-RAE

potential hazards, it is crucial to identify heat stress symptoms in chickens as soon as possible.

Since chickens are homeothermic, high temperatures can affect their capacity to control their body heat, resulting in heat stress that has an adverse effect on their well-being and output. For chickens, the optimal temperature range is between 19 and 22 °C (Pawar et al. 2016). Heat stress can be clearly identified based on the behaviour of chickens. According to the study by Kim et al. (2021), the behaviour, heart rate, and rectal and body surface temperatures are all trustworthy markers for determining the stress level of chickens. The clinical behaviours of heat stress include changes such as in lethargy, reduced food intake, and panting (Lara and Rostagno 2013; Zaboli et al. 2019; Goel 2021; Brugaletta et al. 2022). The manifestations of heat stress in chickens that can be easily observed include open-mouth, panting, and an unusually rapid breathing rate. Chickens experiencing heat stress exhibit these behaviours to reduce their body temperature and cope with high-temperature conditions. In contrast, chickens in a normal state have closed beaks, a stable breathing rate, and do not pant.

The conventional method of identifying heat stress in chickens frequently uses manual techniques, such as monitoring physiological indicators like the body temperature, heart rate, and respiratory rate, observing the behaviour of the birds, and evaluating environmental factors like the temperature and humidity. Numerous research studies have recently demonstrated the high effectiveness of using modern technologies in the challenge of detecting heat stress in chickens. The research of Lin et al. (2018) proposed a model using deep networks and time-lapse images to monitor chicken behaviour, combining the chicken activity with the temperature humidity index (THI) value, which was used as a new predictive indicator for detecting heat stress in chickens. Du et al. (2020) focused on developing a method for extracting vocalisations and a classification system based on the support vector machine (SVM) to assess the chickens' thermal comfort. As a result, the classification performance of the optimal SVM model was 95.1 ± 4.3% (sensitivity) and 97.6 ± 1.9% (precision). Yu et al. (2023) proposed an improved FPN-DenseNet-SOLO model to detect heat stress states in poultry. The recall (0.95), average precision (AP) at an intersection over union (IoU) threshold of 0.5 (AP0.5 = 0.97), at 0.75 IoU (AP0.75 = 0.93), and mean average precision (0.91) of the FPN-DenseNet-SOLO model on the test set were all higher than those of other networks. Bai et al. (2023) proposed an improved Cascade Region-Based Convolutional Neural Network model for heat stress detection, which addressed the issue of inaccurate behaviour recognition when broilers were gathered, with the final average accuracy reaching 88.4%. The study by Solis et al. (2024) proposed using a thermal signature method as a feature extraction tool from temperature matrices obtained from specific areas on the surface of laying hens. This allowed for the development of a computational model to classify different levels of heat stress. The random forest model for the facial region of laying hens achieved the highest performance, with an accuracy of 89.0%.

Figure 1. Heat stressed chickens

Notwithstanding these developments, many of these techniques have a tendency to ignore certain signs of heat stress, like modifications in breathing patterns or other distinctive physiological responses. Rather, they focus mostly on hidden features and general behaviours from deep networks, which produces outcomes that are neither realistic nor objective. Conclusions may be skewed by the absence of a thorough examination of these particular symptoms, which ultimately fails to fairly represent the health conditions of chickens in actual crowded farming settings.

Several research studies (Hao et al. 2022; Elmessery et al. 2023; Qin et al. 2023) have successfully used deep networks with promising results. The application of optical flow algorithms gives extensive information regarding flock and individual chicken interactions, which can play a vital role in developing novel ways for measuring the

https://doi.org/10.17221/46/2025-RAE

well-being and managing poultry (Dawkins et al. 2012). Colles et al. (2016) proposed an optical flow monitoring approach for the identification of Campylobacter infections. Furthermore, other research studies have utilised optical flow analysis techniques to observe chicken behaviour (Dawkins et al. 2009, 2013, 2017; Lee et al. 2010).

This study offers a novel strategy that combines deep network with optical flow, focuses on recognising distinct behaviours and expressions in heat-stressed chickens. In order to more precisely assess heat stress indicators and produce unbiased findings that truly represent the chickens' actual health, a thorough method is suggested.

MATERIAL AND METHODS

Overview

This study proposes a method for detecting heat stress in chickens by identifying open-mouth breathing and panting behaviour. With the input being video footage of chickens, the process of detecting heat stress in chickens involves two phases:

First, a frame is extracted from the video and undergoes open-mouth breathing detection using a deep network. The model returns the locations of the chicken's head and beak if an open-beak is identified.

In the second phase, the chicken's head is treated as a region of interest (ROI) and is combined with the remaining frames to calculate the optical flow vectors. The magnitude of optical flow vectors in the Fourier domain is then used to estimate the main movement frequency. This frequency is compared with the typical panting frequency of chickens to determine if the chicken is panting.

The end result is reached by integrating the outcomes from two phases, as depicted in Figure 2.

Open-mouth breathing detection using deep network

Chickens under heat stress exhibit a protracted and comparatively stable open-mouth breathing pattern, with little variation in the degree of beak opening. One could classify the identification of beak holes as an "Object Detection" challenge. One picture frame serves as the input for this phase. The deep network's task is to automatically identify the chicken's open beak area and the locations of its head and beak regions.

Panting detection via optical flow analysis

The location of the chicken's head – the ROI with an open-mouth breathing in the first phase – as well as the order of the following frames are inputs for this phase. The optical flow vectors within the ROI are computed for every pair of consecutive frames and the ROI. The angle-magnitude filter is then used as a post-processing tool for these vectors. The main frequency of motion in the movie is then ascertained by applying the Fourier transform to the complete set of vectors across each frame. The steps in the pixel motion frequency estimate technique are shown in Figure 3.

Dense optical flow. Optical flow refers to the visible movement pattern of objects within a scene, which is generated by the motion of either the objects themselves, the camera, or both (Shah

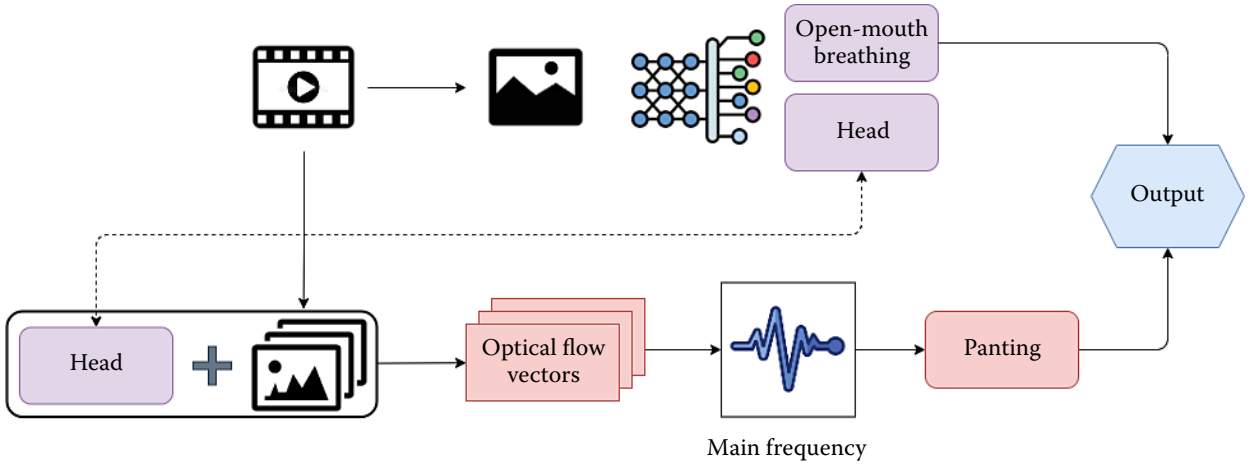

Figure 2. Flowchart of the heat stress detection

https://doi.org/10.17221/46/2025-RAE

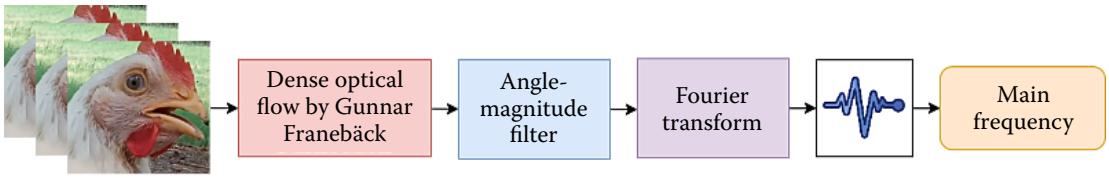

Figure 3. Motion frequency estimation process

and Xuezhi 2021). For a video, the optical flow is defined as a 2D vector field where each vector is a displacement vector representing the movement of pixels from the previous frame to the following frame.

The Gunnar Farnebäck algorithm (Farnebäck 2003) is classified as a method for estimating dense optical flow. It provides a thorough motion estimate by calculating motion vectors for every pixel in a frame, in contrast to sparse methods that concentrate on feature points. The motion of every pixel inside the chicken's head's ROI was ascertained by utilising the Gunnar Farnebäck method.

The displacement magnitude, which represents the motion intensity at each pixel, is conveyed through brightness in the hue, saturation, value (HSV) colour space. The motion direction is encoded as colour in the HSV space. The hue component is calculated using hue = angle/2π and normalised to the range [0, 180]. The saturation component is fixed, while the value component, derived from the magnitude, is normalised to the range [0, 255]. Finally, the HSV colour space is converted to red, green, blue (RGB) for visualisation. Figure 4 presents the optical flow visualisation between frames.

Angle-magnitude filter. The wattle may be used to assess the frequency of the chicken's breathing because it is the component that oscillates the most when it pants. It is perfect for tracking and analysis because of its noticeable motion when panting. Certain situations, as shown in Figure 5, call for extra consideration when figuring out the optical flow vectors because of possible difficulties.

Once the optical flow vectors have been identified, a filtering step is required to keep only the vectors associated with the wattle's movement. This increases the accuracy of determining and estimating the frequency of the chicken's breathing by excluding undesired motions, like those from the backdrop or the chicken's head.

For each optical flow vector, the magnitude is given by Equation (1), and the angle is calculated as Equation (2).

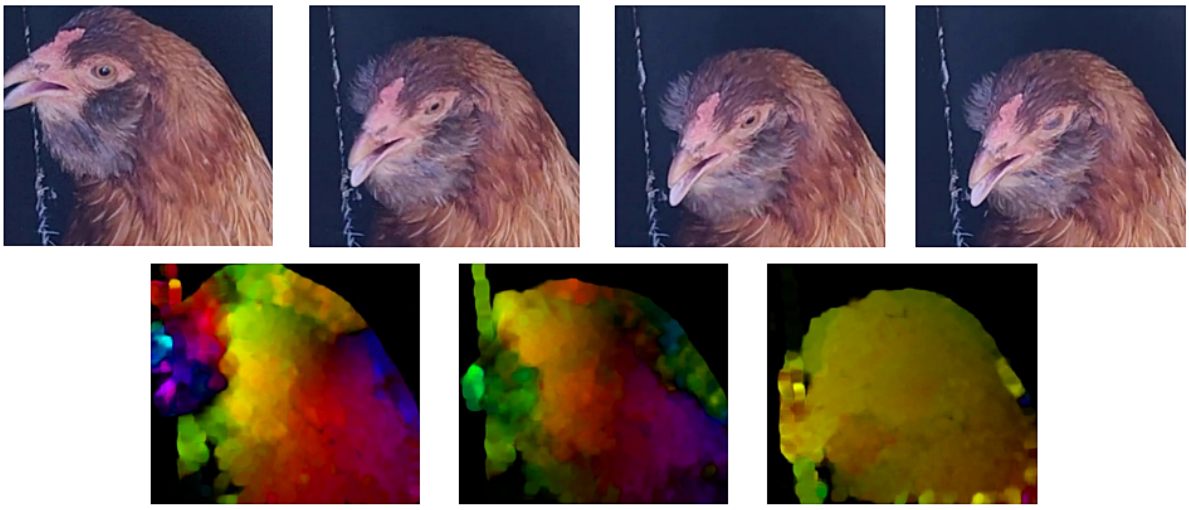

Figure 4. Visualisation of the optical flow results using the hue, saturation, value (HSV) colour space

https://doi.org/10.17221/46/2025-RAE

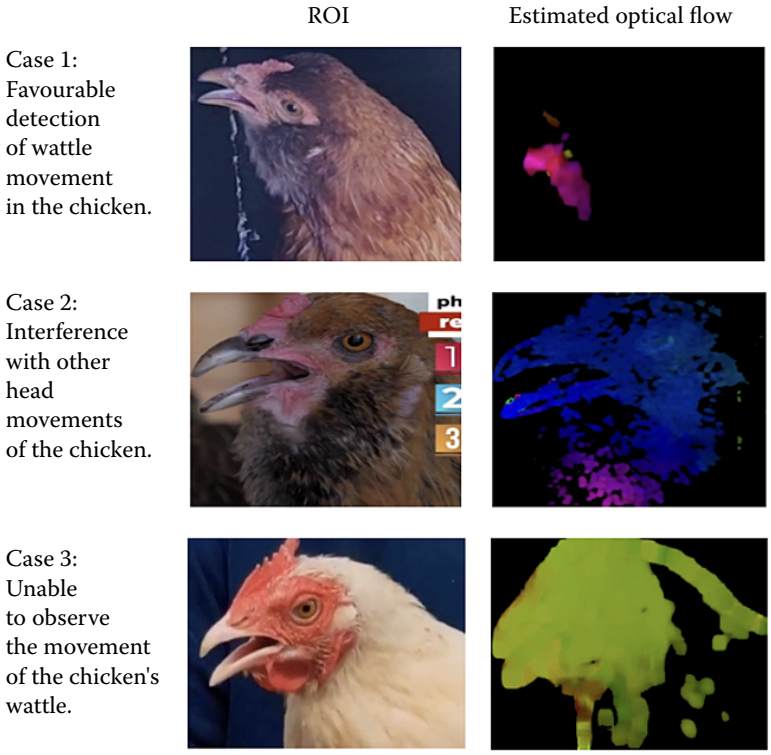

Figure 5. The cases of estimating the wattle movement using optical flow
ROI – region of interest

$$M_i = \sqrt{\left(v_i^x\right)^2 + \left(v_i^y\right)^2} \quad (1)$$

$$\theta_i = \arctan\left(\frac{v_i^y}{v_i^x}\right) \quad (2)$$

where: $v_i = (v_i^x, v_i^y)$ – optical flow vector; M_i – magnitude; θ_i – angle.

The angles are divided into 360 segments, each spanning 1 degree. The number of optical flow vectors within each angular segment is counted. Only the vectors corresponding to angles with a vector count less than the average value are retained.

For the magnitude, the vectors that fall within the top 10% of the highest values are retained because the movements of the chicken's wattle exhibit greater magnitude compared to the background motion and other irrelevant movements. Choosing the top 10% strikes a balance between capturing meaningful movements and excluding noise.

The vectors that satisfy at least one of the two above conditions are used for analysis. Equation (3) represents the general formula, where $\text{threshold}_{\text{top10\%}}$ is the threshold magnitude of the vectors in the top 10%, and average count is the average value of the number of vectors in each angle range.

$$v_i = \begin{cases} v_i, \text{ if } \left(\text{count}\left(\theta_i\right) < \text{average count}\right) \cup \left(M_i > \text{threshold}_{\text{top 10\%}}\right) \\ 0, \text{ otherwise} \end{cases} \quad (3)$$

Fourier transform. The normal respiratory frequency of a chicken ranges from 0.2 to 1.0 Hz (Barnas et al. 1991). However, under heat stress, all the chickens exhibit panting behaviour with a frequency exceeding 250 breaths per minute (Kang et al. 2020), which is approximately 4.17 Hz.

The magnitude values of the optical flow vectors reflect the movements of the chicken's body parts, particularly the wattle, which moves noticeably when the chicken breathes. These movements follow a certain frequency, and gathering the magnitude values provides a discrete signal sequence, suitable for the frequency analysis. The values in the Fourier domain help identify the dominant frequency of the movement (main frequency). When this frequency exceeds a certain threshold (the known panting frequency), it can be inferred that the chicken is panting – a sign of heat stress.

Assume the magnitude signal sequence of the optical flow vectors is $f(t)$, where t represents time. The formula for the Fourier transform of a discrete signal $f(t)$ is given in Equation (4).

https://doi.org/10.17221/46/2025-RAE

$$F(k)=\sum_{n=0}^{N-1} f(n)\times e^{-i2\pi kn/N} \quad (4)$$

where: $F(t)$ – Fourier transform coefficient at frequency index k; N – the number of samples; $f(n)$ – the signal value at time point n; e – the base of the natural logarithm, a mathematical constant approximately equal to 2.71828.

The result is a sequence of complex numbers with both positive and negative frequencies. Only the positive frequencies are used for the analysis. The magnitude of the frequencies obtained from the Fourier transform is calculated in Equation (5).

$$\left|F(k)\right|=\sqrt{Re\left(F(k)\right)^2+Im\left(F(k)\right)^2} \quad (5)$$

where: $Re(F(k))$, $Im(F(k))$ – the real and imaginary parts of the complex number $F(k)$ at frequency f_k, the frequency corresponding to the Fourier transform coefficient $F(k)$.

The optical flow analysis in the frequency domain shows distinct differences between the two cases. When the optical flow vectors in the wattle are clear, the frequency range is higher, and the filter improves frequency analysis. Figure 6 illustrates the results of the vector-to-Fourier transform for these two cases, with and without filtering.

Main frequency. To determine the main frequency, the frequency range is first divided into three intervals:

$F_1=\{f_k \mid 0\le f_k\le 2\text{Hz}\}$, $F_2=\{f_k \mid 2< f_k\le 5\text{Hz}\}$, and

$F_3=\{f_k \mid f_k>5\text{Hz}\}$.

Then, the total magnitude within each frequency interval is calculated. The interval with the highest total magnitude is selected to identify the dominant frequency range. Finally, the average frequency within that interval is calculated to determine the most influential frequency in the sample. The formula used to calculate the main frequency is given by Equation (6).

$$f_{\text{main}}=\frac{\sum_{f_k\in F_{\max}} f_k\times\left|F(k)\right|}{\sum_{f_k\in F_{\max}}\left|F(k)\right|} \quad (6)$$

where: $F_{\max}=\arg\max\left(\sum_{f_k\in F_i}\left|F(k)\right| \mid i\in\{1,2,3\}\right)$

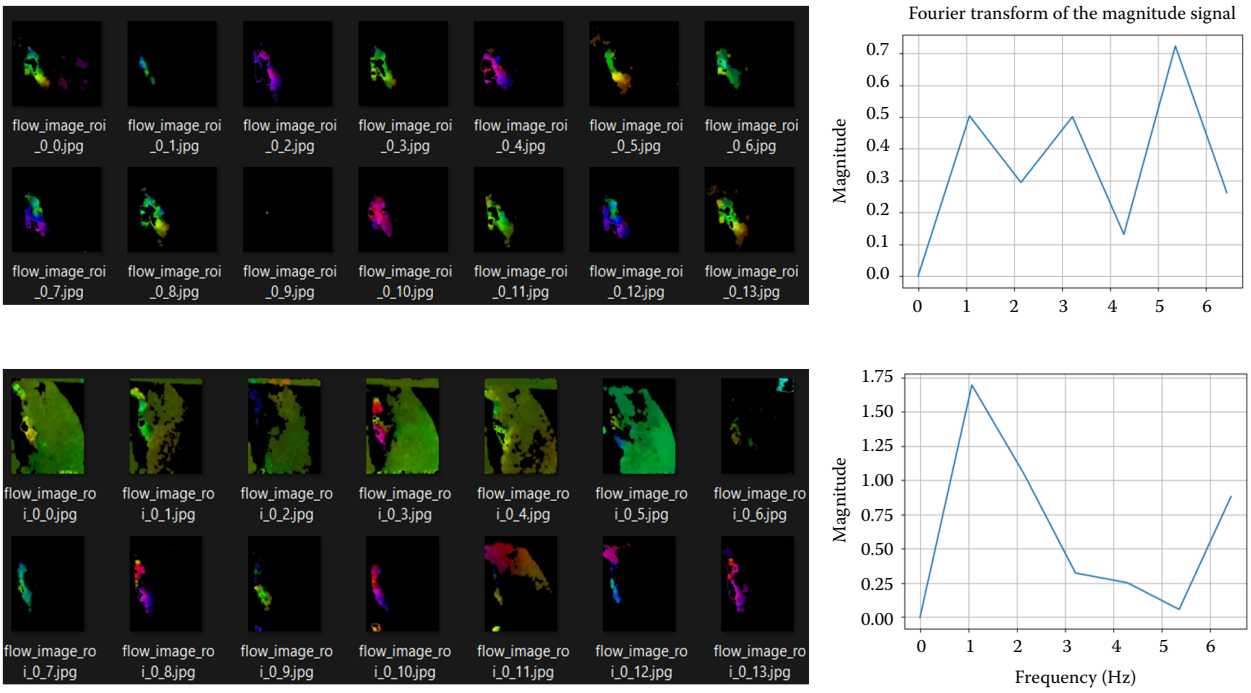

Figure 6. Frequency range obtained during the optical flow vector analysis

https://doi.org/10.17221/46/2025-RAE

Output evaluation metrics

The confidence level of phase 1 is the confidence of the detector, calculated by Equation (7).

$$R_1 = P(\text{Object}) \times \text{IoU} \times P(\text{Class}) \quad (7)$$

where: P(Object) – the probability that the bounding box contains an object; IoU – the "Intersection over Union" between the predicted bounding box and the actual bounding box; P(Class) – the probability that the bounding box contains an object belonging to a specific class.

The formula for the reliability of predictions at phase 2 is determined by Equation (8):

$$R_2 = \frac{N_{\text{filtered}}}{N_{\text{total}}} w_f + \min\left(1, \frac{f_{\text{main}}}{f_{\text{threshold}}}\right) w_t \quad (8)$$

where: R_2– the reliability of the prediction; N_{filtered} – the number of frames after filtering, ensuring that high-quality flow vectors are present; N_{total} – the total number of frames considered within the specified period; f_{main} – the dominant frequency during that period (measured in Hz); $f_{\text{threshold}}$ – the frequency threshold to determine the panting behaviour, defined as 3 Hz.

The threshold of 3 Hz was chosen to help the model detect all the cases of panting in chickens, including those with a slightly lower breathing frequency than 4.17 Hz (250 breaths per minute). Lowering the threshold from 4.17 to 3 Hz helps avoid missing cases of chickens under heat stress that may have a slightly lower breathing frequency, due to factors such as age, stress level, or physiological characteristics. This adjustment allows the model to better adapt to real-world conditions.

The two weights, w_f and w_t are set to 0.5 for the frame ratio and frequency, respectively, allowing for the adjustment of each factor's influence in the reliability calculation process. To assess the overall reliability of the solution, it is essential to consider the uncertainty in each phase. U_1 and U_2 represent the uncertainties of phase 1 and phase 2, respectively, $U_1 = 1 - R_1$; $U_2 = 1 - R_2$.

In Equations (9) and (10), the weights w_1 and w_2 are determined by the uncertainty of each phase, allowing the overall reliability R to be calculated by combining the reliability of both phases.

$$w_1 = \frac{U_2}{U_1 + U_2}, w_2 = \frac{U_1}{U_1 + U_2} \quad (9)$$

$$R = w_1 R_1 + w_2 R_2 \quad (10)$$

Data collection and dataset description

The data used in this study are videos capturing the behaviour of chickens under heat stress, collected from farming environments that include both caged and free-range systems.. The dataset consists of 32 videos. The frame rates, measured in frames per second (FPS) range from 15 to 30, and the resolutions vary from medium to high, ensuring sufficient image quality for the analysis.

A dataset of images was extracted from the frames of these videos, carefully labelled into two classes: "open-mouth breathing" and "head". These images were augmented to enhance their variety. The final dataset is divided into the following: 1 551 image frames for training, 147 image frames for validation and 75 image frames for testing. Figure 7 illustrates some samples from the dataset.

The hyperparameters

In first phase, the You Only Look Once version 11 (YOLOv11) (Khanam and Hussain 2024)

Figure 7. Some samples from the dataset

https://doi.org/10.17221/46/2025-RAE

Table 1. Hyperparameters for training the YOLOv11 pre-trained model

Hyperparameter	Value
Model pre-trained	YOLO11n.pt
Number of layers	319
Parameters	~2.6M
Optimiser	AdamW
Learning rate	0.002
Batch size	16
Epochs	100

architecture is employed alongside the chicken's open-beak region to achieve efficient detection. Table 1 represents the hyperparameters required for training the pre-trained YOLOv11 model, and Table 2 lists the parameters of the Gunnar Farnebäck algorithm. These hyperparameters play a crucial role in tuning the model's learning process, directly affecting its performance in object detection and classification.

The solution presented in this study consists of two phases, where the input of phase 2 is the output of phase 1, so the confidence level in phase 1 must always exceed the threshold of 0.7. To ensure optimal data capture and analysis of the optical flow vectors, the frame rate for phase 2 is set at 15 FPS.

RESULTS

Measures like Precision, Recall, and mAP50 (mean average precision at 0.5 IoU) were employed in this study to assess the deep network's performance. These measures helped gauge the model's accuracy and object identification skills in the classification and detection tasks. The deep network's performance evaluation measures are shown in Table 3. High values were attained by metrics including precision, recall, and mAP50 (with a 0.5 confidence threshold and 0.5 IoU).

Table 3. Evaluation metrics for the deep network

Class	Precision	Recall	mAP50
All class	0.97	0.977	0.988
Head	0.985	0.989	0.993
Open-mouth breathing	0.956	0.966	0.983

mAP50 – mean average precision at 0.5 intersection over union (IoU)

Figure 8 illustrates some prediction results of the model, demonstrating its ability to accurately detect the open-beak state and head position, providing a solid foundation for the analysis in phase 2.

The algorithm achieved nearly 100% detection across all 32 collected videos, consistently identifying heat-stress behaviours with high confidence. Figure 9 shows the average values of the metrics R, R_1 and R_2, calculated for each video.

The average accuracy of the solution was $R = 0.9$, with R_1 achieving 0.8 and R_2 reaching 0.88. These results indicate that both phases of the solution performed well, with phase 2 showing slightly higher accuracy than phase 1. The overall accuracy demonstrates the solution's strong ability to detect

Figure 8. Some prediction results of the deep network

Table 2. Parameters of the Gunnar Farnebäck algorithm

Parameter	Value	Description
pyr_scale	0.5	the image scale to build pyramids for each layer
levels	4	the number of pyramid layers
insize	10	the averaging window size
iterations	10	the number of iterations the algorithm performs at each pyramid level
poly_n	5	size of the pixel neighbourhood used to find the polynomial expansion in each pixel
poly_sigma	1.0	the standard deviation of the Gaussian used to smooth derivatives

https://doi.org/10.17221/46/2025-RAE

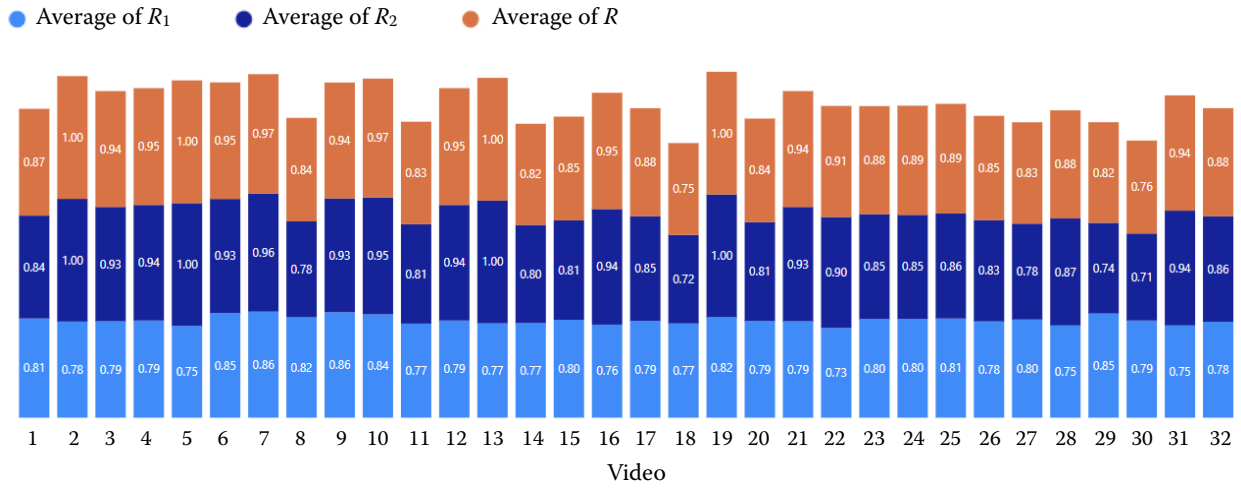

Figure 9. Average of R, R_1 and R_2 by video

R – the overall reliability; R_1 – the confidence level at phase 1; R_2 – the reliability of predictions at phase 2

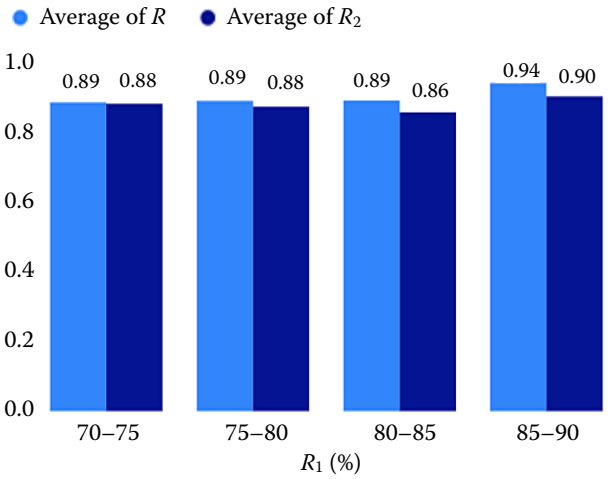

Figure 10. Average of R, R_2 by R_1

R – the overall reliability; R_1 – the confidence level at phase 1; R_2 – the reliability of predictions at phase 2

and analyse heat-stress behaviours in chickens with reliable performance across both phases. Figure 10 illustrates the average values of R, and R_2 based on different ranges of R_1. Specifically, R_1 is divided into four groups: 70–75%, 75–80%, 80–85%, and 85–90%.

The algorithm developed in this study has demonstrated its feasibility and high effectiveness in accurately detecting behaviours of heat stress in chickens, including open-mouth breathing and panting. The outcomes demonstrate the solution's dependability and its ability to precisely identify every case of heat stress in the dataset that was gathered. This demonstrates the method's potential to automate poultry health monitoring, improving farming conditions and reducing the hazards related to heat stress.

DISCUSSION

This study introduced a two-phase method based on visual and motion cues that indicate heat stress. The proposed method demonstrated strong performance in the experimental evaluation. These results are largely due to the method's focus on two key visual indicators of heat stress – open-mouth breathing and panting – which are distinctive and can be effectively captured using image and motion analysis. Although a direct comparison is difficult due to differences in the datasets and approaches, this method achieved high metrics indicating its potential for the accurate and robust heat stress identification in practical settings. Table 4 presents an overview of selected studies related to poultry behaviour and welfare monitoring, offering context for the current approach.

One notable strength of the system lies in its ability to function effectively when chickens appear clearly in front of the camera. This is because both the detection and the optical flow estimation phases rely on clear visual cues. However, unlike dead chickens, which tend to be displaced toward the front area by the flock, heat-stressed chickens do not exhibit such movement patterns. As a result, although the system performs effectively under crowded conditions when heat-stressed chickens appear in front of the camera, it may fail to detect

https://doi.org/10.17221/46/2025-RAE

Table 4. Overview of studies related to poultry behaviour analysis and heat stress detection

Study	Method/technology	Focus/feature	Performance/outcome
Du et al. (2020)	SVM classification of vocalisations	chicken vocal signals & thermal comfort	sensitivity: 95.1% ± 4.3; precision: 97.6% ± 1.9
Yu et al. (2023)	improved FPN-DenseNet-SOLO model	heat stress detection using object detection	recall: 0.95; AP@0.5: 0.97; AP@0.75: 0.93; mAP: 0.91
Dawkins et al. (2009, 2013, 2017); Lee et al. (2010)	optical flow analysis	flock movement, behaviour, and welfare monitoring	not quantified for heat stress; general behaviour analysis
The proposed method	deep network & optical flow	detect visible signs & behaviour of heat-stressed chickens	high performance (metrics reported in subsection Results)

SVM – support vector machine

those remaining within the inner area of the flock or under occlusion. This remains a challenge for vision-based systems in highly dense environments and highlights the need for further improvements.

Future research could focus on incorporating temporal consistency across frames to infer the presence of heat-stressed chickens even when they are partially hidden. Additionally, collecting more data from various camera angles – such as top-view or oblique views – may help reduce the occlusion and improve the detection coverage in practical farm environments.

CONCLUSION

Through the use of deep networks and optical flow, this study contributed to a novel technique for automatically identifying heat-stressed behaviours in crowded conditions. The open-mouth breathing of the chickens was detected using a deep network, and the frequency of their breathing was analysed using optical flow and Fourier transform to identify panting, a crucial sign of heat stress. Through the integration of open-mouth breathing behaviour and panting frequency, the two-phase technique improves efficiency, lowers noise, and guarantees robust, reliable heat stress detection. The experimental results demonstrated high accuracy, with the metrics R, R_1 and R_2, averaging 0.90, 0.80, and 0.88, respectively, proving the feasibility and effectiveness of the proposed method in recognising heat stress.

This approach opens up new avenues for the automatic monitoring of poultry health in practical farming environments, contributing to improved farming conditions and reducing the negative impacts of heat stress. This automated monitoring solution also helps reduce reliance on manual monitoring methods while enhancing the sustainability and efficiency of the poultry industry.

REFERENCES

Abbas G., Arshad M., Tanveer A.J., Jabbar M.A., Arshad M., Al-Taey D.K.A., Mahmood A., Khan M.A., Imran M.S., Khan A.A., Konca Y., Sultan Z., Qureshi R.A.M., Iqbal A., Amad F., Ashraf M., Asif M., Abbas S., Mahmood R., Abbas H., Mohyuddin S.G., Jiang M.Y. (2022): Combating heat stress in laying hens a review. Pakistan Journal of Science, 73: 633–655.

Bai Y., Zhang J., Chen Y., Yao H., Xin C., Wang S., Yu J., Chen C., Xiao M., Zou X. (2023): Research into heat stress behavior recognition and evaluation index for yellow-feathered broilers, based on improved cascade region-based convolutional neural network. Agriculture, 13: 1114.

Barnas G.M., Hempleman S.C., Harinath P., Baptise J.W. (1991): Respiratory system mechanical behavior in the chicken. Respiration Physiology, 84: 145–157.

Brugaletta G., Teyssier J.-R., Rochell S.J., Dridi S., Sirri F. (2022): A review of heat stress in chickens. Part I: Insights into physiology and gut health. Frontiers in Physiology, 13: 934381.

Colles F.M., Cain R.J., Nickson T., Smith A.L., Roberts S.J., Maiden M.C.J., Lunn D., Dawkins M.S. (2016): Monitoring chicken flock behaviour provides early warning of infection by human pathogen Campylobacter. Proceedings of the Royal Society B: Biological Sciences, 283: 20152323.

Dawkins M.S., Lee H.-J., Waitt C.D., Roberts S.J. (2009): Optical flow patterns in broiler chicken flocks as automated measures of behaviour and gait. Applied Animal Behaviour Science, 119: 203–209.

Dawkins M.S., Cain R., Roberts S.J. (2012): Optical flow, flock behaviour and chicken welfare. Animal Behaviour, 84: 219–223.

https://doi.org/10.17221/46/2025-RAE

Dawkins M.S., Cain R., Merelie K., Roberts S.J. (2013): In search of the behavioural correlates of optical flow patterns in the automated assessment of broiler chicken welfare. Applied Animal Behaviour Science, 145: 44–50.

Dawkins M.S., Roberts S.J., Cain R.J., Nickson T., Donnelly C.A. (2017): Early warning of footpad dermatitis and hockburn in broiler chicken flocks using optical flow, bodyweight and water consumption. Veterinary Record, 180: 499–499.

Du X., Carpentier L., Teng G., Liu M., Wang C., Norton T. (2020): Assessment of laying hens' thermal comfort using sound technology. Sensors, 20: 473.

Elmessery W.M., Gutiérrez J., Abd El-Wahhab G.G., Elkhaiat I.A., El-Soaly I.S., Alhag S.K., Al-Shuraym L.A., Akela M.A., Moghanm F.S., Abdelshafie M.F. (2023): YOLO-based model for automatic detection of broiler pathological phenomena through visual and thermal images in intensive poultry houses. Agriculture, 13: 1527.

Farnebäck G. (2003): Two-frame motion estimation based on polynomial expansion. In: Image Analysis. Berlin, Heidelberg, Springer: 363–370.

Franzo G., Legnardi M., Faustini G., Tucciarone C., Cecchinato M. (2023): When everything becomes bigger: Big data for big poultry production. Animals, 13: 1804.

Goel A. (2021): Heat stress management in poultry. Journal of Animal Physiology and Animal Nutrition, 105: 1136–1145.

Hao H., Fang P., Duan E., Yang Z., Wang L., Wang H. (2022): A dead broiler inspection system for large-scale breeding farms based on deep learning. Agriculture, 12: 1176.

Kang S., Kim D.-H., Lee S., Lee T., Lee K.-W., Chang H.-H., Moon B., Ayasan T., Choi Y.-H. (2020): An acute, rather than progressive, increase in temperature-humidity index has severe effects on mortality in laying hens. Frontiers in Veterinary Science, 7: 568093.

Khanam R., Hussain M. (2024): YOLOv11: An Overview of the Key Architectural Enhancements. arXiv: 2410.17725 [cs.CV]. Available at https://arxiv.org/abs/2410.17725.

Kim D.-H., Lee Y.-K., Lee S.-D., Kim S.-H., Lee K.-W. (2021): Physiological and behavioral responses of laying hens exposed to long-term high temperature. Journal of Thermal Biology, 99: 103017.

Kim H.-R., Ryu C., Lee S.-D., Cho J.-H., Kang H. (2024): Effects of heat stress on the laying performance, egg quality, and physiological response of laying hens. Animals, 14: 1076.

Lara L., Rostagno M. (2013): Impact of heat stress on poultry production. Animals, 3: 356–369.

Lee H.-J., Roberts S.J., Drake K.A., Dawkins M.S. (2010): Prediction of feather damage in laying hens using optical flows and Markov models. Journal of The Royal Society Interface, 8: 489–499.

Lin C.-Y., Hsieh K.-W., Tsai Y.-C., Kuo Y.-F. (2018): Monitoring chicken heat stress using deep convolutional neural networks. In: 2018 ASABE Annual International Meeting, American Society of Agricultural and Biological Engineers, 2018: 1800314.

Pawar S.S., Basavaraj S., Dhansing L.V., Pandurang K.N., Sahebrao K.A., Vitthal N.A., Pandit B.M., Kumar B.S. (2016): Assessing and mitigating the impact of heat stress in poultry. Advances in Animal and Veterinary Sciences, 4: 332–341.

Qin X., Lai C., Pan Z., Xiang Y., Wang Y. (2023): Recognition of abnormal-laying hens based on fast continuous wavelet and deep learning using hyperspectral images. Sensors, 23: 3645.

Shah S.T.H., Xuezhi X. (2021): Traditional and modern strategies for optical flow: An investigation. SN Applied Sciences, 3: 289.

Solis I.L., de Oliveira-Boreli F.P., de Sousa R.V., Martello L.S., Pereira D.F. (2024): Using thermal signature to evaluate heat stress levels in laying hens with a machine-learning-based classifier. Animals, 14: 1996.

Yu Z., Liu L., Jiao H., Chen J., Chen Z., Song Z., Lin H., Tian F. (2023): Leveraging SOLOv2 model to detect heat stress of poultry in complex environments. Frontiers in Veterinary Science, 9: 1062559.

Zaboli G., Huang X., Feng X., Ahn D.U. (2019): How can heat stress affect chicken meat quality? – A review. Poultry Science 98: 1551–1556.

Received: April 12, 2025
Accepted: July 16, 2025
Published online: October 9, 2025